

Philipp Mohr and Gerhard Bauch are with the Institute of Communications, Hamburg University of Technology, Hamburg, 21073, Germany. E-mail: {philipp.mohr; bauch}@tuhh.de.

### B. Node Operations

We introduce the discrete random variables  $T_j^{ch}$ ,  $T_m^v$  and  $T_n^c$  for modeling the channel, VN and CN messages. A realization  $t_n^c$  of  $T_n^c$  takes values from an LLR-sorted alphabet  $\mathcal{T}_\triangleright^c = \{\pm 1, \dots, \pm 2^{w_\triangleright-1}\} = \{-2^{w_\triangleright-1}, \dots, -1, 1, \dots, 2^{w_\triangleright-1}\}$  where  $\triangleright \in \{ch, v, c\}$  and  $\triangleright \in \{j, m, n\}$ . We set  $w_{ch}=5$  and  $w_v=w_c=w$  in this paper. For the design of the decoder, we keep track of  $p(x_m, t_m^v)$  and  $p(x_n, t_n^c)$  that change with every VN and CN update. Updating a VN memory location  $m \in \mathcal{U}^v$  yields [11]

$$y_m^v = L(x_m | t_{\text{col}(m)}^{ch}) + \sum_{n \in \xi_m^v} \bar{L}(t_n^c | x_m) \quad (2)$$

with extrinsic CN locations  $\xi_m^v = (n: n \neq m, \text{col}(n) = \text{col}(m))$ . An LLR reconstruction of a message  $t_n^c$  is denoted as  $\bar{L}(t_n^c | x) = \log p(\bar{T}_n^c = t_n^c | x=0) / p(\bar{T}_n^c = t_n^c | x=1)$  using the aligned variables  $\bar{T}_n^c$  introduced in the next subsection II-C. The hard decision yields  $\hat{x}_m = (1 - \text{sgn}(\hat{L}_m)) / 2$  with the a-posteriori probability (APP) LLR  $\hat{L}_m = y_m^v + \bar{L}(t_m^c | x_m)$ . Row-layered decoder structures, such as the one in Fig. 8, typically use the APP LLR for computing (2) efficiently as  $y_m^v = \hat{L}_m - \bar{L}(t_m^c | x_m)$ . Those decoders initialize the APP LLR with  $\hat{L}_m = L(x_m | t_{\text{col}(m)}^{ch})$ . Hence, the reconstruction of the channel message must be done only once for all iterations. In an implementation the reconstruction in (2) is typically carried out with integer scaled LLRs of bit width  $w' \approx 8$  to avoid performance loss [11].

Updating a CN memory location  $n \in \mathcal{U}^c$ , exploiting the minimum-approximation [3], yields [11]

$$t_n^c = Q(y_n^c) \text{ with } y_n^c = \prod_{m \in \xi_n^c} \text{sgn}(y_m^v) \min_{m \in \xi_n^c} |y_m^v| \quad (3)$$

with extrinsic VN locations  $\xi_n^c = (m: m \neq n, \text{row}(m) = \text{row}(n))$ . Without performance loss, the quantizer  $Q$  can be moved before the CN update (cf. Fig. 2a & 2b) lowering complexity.

### C. Alignment Regions

The reconstruction  $\bar{L}(t_n^c | x)$  in (2) and quantization  $Q: \mathcal{Y}_n^c \rightarrow \mathcal{T}_n^c$  in (3) can be designed such that decoding messages from different memory locations  $n$  can share the same functions. Using the same functions reduces the overall number of parameters to be designed and implemented. Common functions are realized through an alignment operation applied to the variables  $T_n^c$  and  $X_n$  before the node design as [11]

$$\bar{T}_n^c = \frac{1}{|\mathcal{A}_n|} \sum_{n' \in \mathcal{A}_n} T_{n'}^c \text{ and } \bar{X}_n = \frac{1}{|\mathcal{A}_n|} \sum_{n' \in \mathcal{A}_n} X_{n'} \quad (4)$$

where  $\mathcal{A}_n$  comprises all elements from the same region. This work considers a row-alignment  $\mathcal{A}_n = \{n': \text{row}(n') = \text{row}(n)\}$  or matrix-alignment  $\mathcal{A}_n = \mathcal{N}$  [11].

### D. Region-Specific Quantization with Check Node Awareness

A compact version of the CN messages can be obtained with threshold quantization  $t_n^c = Q(y_n^c)$  (cf. Fig. 2a). The objective is to maximize the mutual information  $\max_Q I(\bar{X}_n; \bar{T}_n^c)$  preserved by any CN message in the

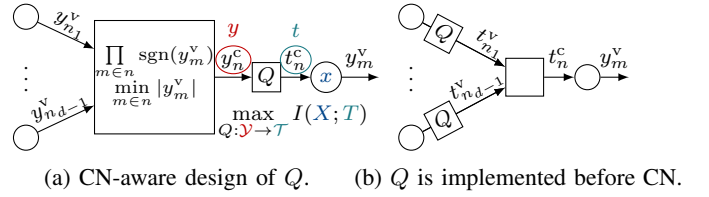


Fig. 2: Structure (a) is used during the design phase and structure (b) is used in the implementation.

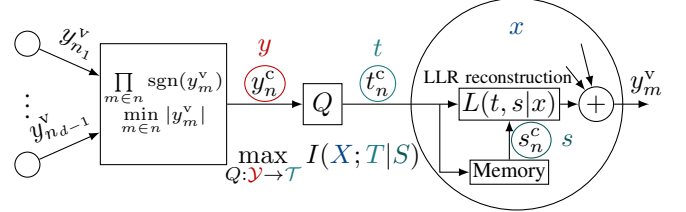


Fig. 3: Quantizer design with memory-assisted reconstruction.

alignment region  $\mathcal{A}_n$ . The optimization of  $Q$  can be performed with the sequential IB algorithm [8], also described in section IV. This algorithm requires the distribution  $p(\bar{x}_n, \bar{y}_n^c) = \sum_{n' \in \mathcal{A}_n} p(x_{n'}, Y_{n'}^c = \bar{y}_n^c) / |\mathcal{A}_n|$ . In case of a layered schedule, each update points to a subset of all memory locations  $\mathcal{U} \subset \mathcal{N}$ . A single quantizer design suffices for each region  $\mathcal{N}_a = \{\mathcal{A}_n: n \in \mathcal{U}\}$  where  $a \in \{1, \dots, |\mathcal{A}|\}$  enumerates the distinct regions. The notation  $\{\mathcal{A}_n: n \in \mathcal{U}\}$  builds a set with unique elements, e.g.,  $\{\{1, 2\}, \{2, 1\}, \dots\}$  reduces to  $\{\{1, 2\}, \dots\}$ . The quantizer designed for region  $\mathcal{N}_a$  is used only for updating the locations defined by  $\mathcal{N}_a \cap \mathcal{U}$  [11].

### III. MEMORY-ASSISTED RECONSTRUCTION

A small bit width  $w$  of the exchanged messages significantly lowers the decoder complexity for several reasons:

- One quantization operation uses  $w-1$  comparisons [10].
- The routing network size scales with  $w$ .
- The min-CN update can be carried out much faster. For example using  $w=2$  instead of  $w=3$  bits potentially reduces the logic gate delay by a factor of 4 [10].

Unfortunately, with  $w=2$  bit these major complexity savings can lead to a noticeable performance degradation [11]. This section proposes a novel approach to overcome most of the degradation when using e.g.  $w=2$  instead of  $w=3$  bits. Fig. 3 extends the setup by preserving the old CN message  $t_n^c$  of the previous iteration as  $s_n^c$ . We remark that preserving  $s_n^c$  for another iteration would give only marginal performance gains.

#### A. Modification of Existing Decoder Design

Instead of aiming for  $\max_Q I(\bar{X}; \bar{T}_n^c)$  we propose to take the statistics of the message  $s_n^c$  into account. The message  $s_n^c$  already provides a certain amount of mutual information  $I(X_n^c; S_n^c)$ . The optimization of the quantizer shall optimize preservation of additional mutual information  $\max_Q I(X_n^c; T_n^c | S_n^c)$ . The variable node update now takes into account  $s_n^c$  as

$$y_m^v = L(x_m | t_{\text{col}(m)}^{ch}) + \sum_{n \in \xi_m^v} \bar{L}(t_n^c, s_n^c | x_m) \quad (5)$$

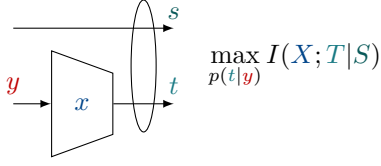


Fig. 4: Information bottleneck setup with side information.

For the design of  $Q: \mathcal{Y}_n^c \rightarrow \mathcal{T}_n^c$  in (3) we measure the joint distribution  $p(x_n, y_n^c, s_n^c)$  which considers correlations between  $t_n^c$  and  $s_n^c$ . Therefore, we generate a large set of decoding messages  $x_n, y_n^c, s_n^c$  under a specific design- $E_b/N_0$ . In the next section IV we introduce a side-information aware IB algorithm which is used for optimization of the quantization thresholds. We define  $X_n, Z_n^c, T_n^c$ , and  $S_n^c$  as the relevant, observed, compressed and side-information variable,  $X, Y, T$ , and  $S$ , respectively. The optimization aims for  $\max_{p(t|y)} I(X; T|S)$ . We remark that the alphabet  $\mathcal{Y}$  is not strictly LLR-sorted as defined in (7) as a result of the CN minimum approximation.

#### IV. INFORMATION BOTTLENECK ALGORITHM WITH SIDE-INFORMATION AWARENESS

Typically, an IB setup is defined by a relevant, observed and compressed random discrete variable  $X, x \in \mathcal{X} = \{0, 1\}$ ,  $Y, y \in \mathcal{Y} \in \{1, \dots, |\mathcal{Y}|\}$  and  $T, t \in \mathcal{T} = \{1, \dots, |\mathcal{T}|\}$  that form a Markov chain  $X \rightarrow Y \rightarrow T$ . The IB method is a generic clustering framework for designing compression operations  $p(t|y)$  with optimization objective  $\max_{p(t|y)} I(X; T) - \beta^{-1} I(Y; T)$ . The choice of  $\beta \geq 0$  allows to trade preservation of relevant information  $I(X; T)$  for compression. Of very high practical interest is the case where  $\beta \rightarrow \infty$  because it can be achieved with a deterministic mapping through threshold quantization

$$t = Q(y) = \mathcal{T}[k] \quad \tau_k \leq y < \tau_{k+1}, 0 \leq k < |\mathcal{T}| \quad (6)$$

with outer thresholds  $\tau_0 = 0$  and  $\tau_{|\mathcal{T}|} = |\mathcal{Y}|$ , and  $\mathcal{T}[k]$  identifying the  $k$ th element of the ordered set  $\mathcal{T}$ . The mapping with thresholds can be information-optimum if [14]

$$L(x|y=1) \leq L(x|y=2) \leq \dots \leq L(x|y=|\mathcal{Y}|). \quad (7)$$

This section extends the conventional setup with a fourth variable  $S$  which provides side-information about  $X$  [13], see Fig. 4. Prior works [12], [13] also consider a setup with side information, however, those works do not explicitly provide a low-complexity solution for optimizing a threshold quantizer in the context of LDPC decoding. We propose Algorithm 1 which is a modified variant of the sequential IB algorithm from [8] taking into account the side information  $S$ . The algorithm exploits (7) to sequentially optimize initial random boundaries  $\tau_k$  defining the target clusters  $\mathcal{Y}_t = \{y: \tau_t \leq y < \tau_{t+1}\} \subset \mathcal{Y}$ . To avoid local optima, we run 500 different initializations in parallel. We enforce symmetric thresholds  $\tau_k = |\mathcal{T}| - \tau_{|\mathcal{T}| - k}$ , reducing the number of design and implementation parameters.

##### A. Merger Costs with Side Information

In line 14, the element  $y$  and counterpart element  $y'$  are moved into singleton clusters  $\mathcal{Y}_{|\mathcal{T}|+1}$  and  $\mathcal{Y}_{|\mathcal{T}|+2}$ , respectively. The temporary decompression is modeled with a discrete random variable  $\tilde{T}, \tilde{t} \in \tilde{\mathcal{T}} = \mathcal{T} \cup \{|\mathcal{T}|+1, |\mathcal{T}|+2\}$ . Line 16 optimizes

**Algorithm 1** A sequential IB algorithm from [8] considering side information  $s$  in the merger cost computation (line 16).

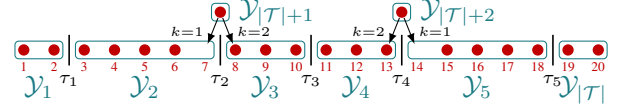
**Input:**  $p(x, y, s), |\mathcal{T}|$

**Output:**  $p(t|y), p(x, t, s)$

- 1: Create random symmetric clustering  $p(t|y)$ ;
- 2: Compute  $p(x, t, s) = \sum_y p(t|y)p(x, y, s)$ ;
- 3: Extend clusters  $\mathcal{Y}_1, \dots, \mathcal{Y}_{|\mathcal{T}|}$  with empty singleton clusters  $\mathcal{Y}_{|\mathcal{T}|+1}$  and  $\mathcal{Y}_{|\mathcal{T}|+2}$ ;
- 4: **repeat**
- 5:   Save  $p(t|y)$  as  $p^{\text{old}}(t|y)$ ;
- 6:   **for**  $t \in \{1, \dots, |\mathcal{T}|/2 - 1\}$  **do**
- 7:     **for**  $(t_1, t_2) \in \{(t, t+1), (t+1, t)\}$  **do**
- 8:       **repeat**
- 9:         **if**  $t_1 == t$  **then**
- 10:           $y$  is rightmost element in cluster  $\mathcal{Y}_{t_1}$ ;
- 11:         **else if**  $t_1 == t+1$  **then**
- 12:           $y$  is leftmost element in cluster  $\mathcal{Y}_{t_1}$ ;
- 13:         **end if**
- 14:         Move  $y$  into  $\mathcal{Y}_{|\mathcal{T}|+1}$ , and  $y' = |\mathcal{Y}| + 1 - y$  into  $\mathcal{Y}_{|\mathcal{T}|+2}$ ;
- 15:         Update  $p(x, t, s)$ ;
- 16:         Compute optimal cluster using (12):

$$k = \arg \min_{k^* \in \{1, 2\}} C_{\text{sym}}(y, k^*) \quad (8)$$

Example:  $|\mathcal{Y}|=20, |\mathcal{T}|=6, t=2, (t_1, t_2)=(2, 3), y=7, y'=14$



- 17:       Merge  $\mathcal{Y}_{|\mathcal{T}|+1}$  into  $\mathcal{Y}_{t_k}$ , and  $\mathcal{Y}_{|\mathcal{T}|+2}$  into  $\mathcal{Y}_{|\mathcal{T}|+1-t_k}$ ;
- 18:       Update  $p(x, t, s)$  and  $p(t|y)$ ;
- 19:       **until**  $t_k == t_1$
- 20:     **end for**
- 21:   **end for**
- 22: **until**  $p(t|y) == p^{\text{old}}(t|y)$
- 23: **return**  $p(t|y), p(x, t, s)$

the deterministic mapping  $p(t|\tilde{t}) = \delta(t - f_k(\tilde{t}))$  with  $f_k: \tilde{\mathcal{T}} \rightarrow \mathcal{T}$ . The algorithm restricts merging  $y$  into an adjacent cluster  $t_1$  or  $t_2$ . Thus, two mapping options exist  $k \in \{1, 2\}$  with

$$f_k(\tilde{t}) = \begin{cases} \tilde{t} & \tilde{t} \in \mathcal{T} \\ t_k & \tilde{t} = |\mathcal{T}|+1 \\ t'_k & \tilde{t} = |\mathcal{T}|+2 \end{cases} \quad \text{with } t'_k = |\mathcal{T}|+1 - t_k. \quad (9)$$

The mutual information loss from merging is

$$C_{\text{sym}}(y, k) = I(X; \tilde{T}|S) - I(X; T|S) \quad (10)$$

$$= \sum_{\tilde{t}, s} p(\tilde{t}, s) D_{\text{KL}}(p(x|\tilde{t}, s) || p(x|f_k(\tilde{t}), s)) \quad (11)$$

$$= \sum_s p(s) (C(y, t_k|s) + C(y', t'_k|s)) \quad (12)$$

where the individual merger costs are

$$C(y, t|s) = p(\tilde{T} = t|s) D_{\text{KL}} \left\{ p(x|\tilde{T} = t, s) || p(x|T = t, s) \right\} + p(Y = y|s) D_{\text{KL}} \left\{ p(x|Y = y, s) || p(x|T = t, s) \right\} \quad (13)$$

with  $D_{\text{KL}}(p||q) = \sum_x p(x) \log_2(p(x)/q(x))$ .

#### V. EVALUATION WITH 5G CODES

This section investigates the performance of the proposed decoders with memory-assistance. As in [11] we use a 5G-LDPC code with length 8448, base graph 1 and various code rates [1]. Furthermore, we consider an AWGN channel with

BPSK modulation. All decoders use the initialization schedule described in [11] to avoid useless CN updates resulting from processing punctured messages. If not mentioned otherwise, the remaining schedule follows the flooding scheme with a maximum of 30 decoder iterations. Each decoder design uses a large set of training data with 10000 transmitted and received code words generated for a specific design  $E_b/N_0$ . Analytical tracking of joint probabilities for the design of memory-assisted decoders seems infeasible. For a fair comparison, also the conventional decoders are designed with the training data, leading to slightly different results compared to our work [11].

#### A. Evolution of Mutual Information

Fig. 5 depicts the evolution of mutual information between code bit  $X$  and the corresponding hard decision  $\hat{X}$  for every iteration. The quantized messages are matrix-aligned such that all messages use the same alphabet of reliability levels in one iteration. The design process is initialized with the same design  $E_b/N_0$ . Particularly under 2-bit decoding, the mutual information gains per iteration are significantly improved with the proposed memory-assistance. For 3-bit decoding those gains appear smaller. Nevertheless, the proposed 3-bit decoding almost achieves the same performance as the conventional 4-bit decoding.

#### B. Boundary Placement for Memory-Assisted Reconstruction

This section analyzes the placement of quantizer boundaries  $\tau_k$  for every iteration to explain the performance gains achieved with the proposed structure. Now, all decoders use an individual design- $E_b/N_0$  so that the mutual information converges after 30 iterations  $I(X, \hat{X})(30) \approx 0.9999$ . A careful optimization is very important to ensure minimum frame error rate for a given budget of decoding iterations.

Fig. 6 shows boundary levels which increase for higher iterations as the reliability of messages improves. One key observation is that boundary magnitudes for the proposed 2-bit decoder show up an alternating rising and falling trend. Thus, memory-assistance enhances the resolution by using different quantizers in successive iterations. This behavior clearly shows the effectiveness of the side-information aware IB algorithm: A CN message  $t$  is a compressed version of the non-quantized LLR  $y_n^c$  in (3) from the current iteration. A CN message  $s$  is a compressed version of  $y_n^c$  from the previous iteration. The difference  $\Delta y_n^c = y_n^c - y_n^c$  is sufficiently small on average, such that  $s$  can approximately resolve  $y_n^c$ . Different boundaries for  $s$  and  $t$  improve their combined capability to resolve  $y^c$  in *relevant ranges*. The combined resolution approaches the 3-bit quantizer in Fig. 6.

We remark that the side information  $s$  is only actively used during reconstruction  $L(t, s|x)$ . For example, consider a sign-magnitude alphabet sorted by underlying LLR with  $t \in \mathcal{T} = \{-2, -1, +1, +2\}$ . For  $t = +2$  the reconstructed LLR  $L(t = +2, s|x)$  is more reliable if the message in memory is matching, e.g.,  $s = +2$ . It is less reliable if  $s$  does not agree, e.g.,  $s = -2$ . Thus,  $L(t = +2, s = +2|x) > L(t = +2, s = -2|x)$ . Combined knowledge about the message  $s$  and  $t$  allows better inference of the non-quantized LLR  $y_n^c$ .

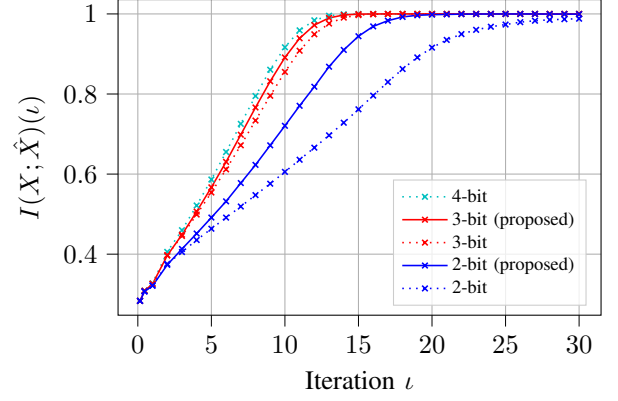


Fig. 5: Evolution of mutual information with code rate 1/3. All results obtained with same design  $E_b/N_0 = 1.0$  dB.

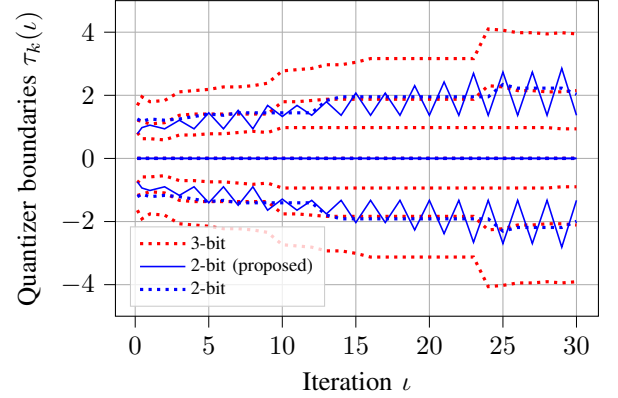


Fig. 6: Evolution of boundary placement each with code rate 1/3 and individual design  $E_b/N_0 = .55, .73$  and  $1.0$  dB.

#### C. Reduced Complexity with Merged Check Node Messages

In the previous sections the side information  $s^c$  is equal to  $t^c$  from the previous iteration and is discarded after it has been used. Instead of discarding  $s^c$ , this section considers a side information  $s^\Psi \in \{\pm 1, \dots, \pm 2^{w_\Psi-1}\}$  which is merged with  $t^c$  into a compressed message  $t^\Upsilon = \Upsilon(s^\Psi, t^c) \in \{\pm 1, \dots, \pm 2^{w_\Upsilon-1}\}$  obtained through a compression table  $\Upsilon$ . The table is designed using the IB method with a measured joint distribution  $p(x, s^\Psi, t^c)$ . The reconstruction in (5) now uses  $\hat{L}(t^\Upsilon|x)$  instead of  $\hat{L}(s^\Psi, t^c|x)$ . The side information can propagate over many iterations as  $s^\Psi = \Psi(\Upsilon(s^\Psi, t^c))$  where  $\Psi$  is another compression for reducing the table size of  $\Upsilon$ .

The compression reduces the memory demand from  $|\mathcal{N}|(w_\Psi + w_c)$  to  $|\mathcal{N}|w_\Upsilon$  bits in a row-layered decoder structure depicted in Fig. 8. The row-layered schedule sequentially updates orthogonal sets of rows of  $\mathbf{H}$  [11]. One layer update consists of partial VN and a full CN update (see section II-B). A partial VN update computes the VN-to-CN message as  $t^v = Q(L^v)$  with  $L^v = \hat{L} - \hat{L}^c$ . The reconstruction  $\hat{L}^c = \phi(t^\Upsilon)$  translates  $t^\Upsilon$  from the previous iteration to a  $w'$ -bit integer representations of  $\hat{L}(t^\Upsilon|x)$ . Significant loss is avoided if  $w' \geq 7$  bits [11]. A permutation performs a cyclic shift of  $Z$  parallel messages. A full CN update computes CN-to-VN messages for all connected VNs according to (3). After an inverse permutation, a CN-to-VN message  $t^v$  is merged with the side information  $s^\Psi$ . Finally,  $\hat{L} = L^v + \phi(t^\Upsilon)$ .



